

Band offsets from two special GaAs-Al_xGa_{1-x}As quantum-well structures

R. C. Miller, A. C. Gossard, and D. A. Kleinman
 AT&T Bell Laboratories, Murray Hill, New Jersey 07974
 (Received 22 April 1985)

Half-parabolic quantum wells and two-stepped quantum wells have been grown by molecular-beam epitaxy with the GaAs-Al_xGa_{1-x}As system and investigated by photoluminescence techniques to determine the band offsets at the heterointerfaces. Both structures provide interband transitions that are sensitive to the partitioning of the energy-gap discontinuity $\Delta E_g = \Delta E_c + \Delta E_v$ between the conduction and valence bands. It is concluded that the data require valence-band offsets ΔE_v equal to 38% and 41% of ΔE_g for the half-parabolic wells and the two-stepped wells, respectively. These band offsets are therefore in agreement with the trend of other recent determinations.

I. INTRODUCTION

Previous work has shown the importance of off-diagonal exciton transitions ($\Delta n \neq 0$) and certain types of structures for the determination of the band offsets for GaAs-Al_xGa_{1-x}As quantum wells.^{1,2} This Brief Report describes the estimation of these band offsets from photoluminescence studies of two new GaAs quantum-well structures, in particular, half-parabolic wells (HPW) and symmetric two-stepped wells (TSW). These structures were designed to provide transitions sensitive to the band offsets. The photoluminescence results show that the valence-band offset $\Delta E_v \approx Q_v \Delta E_g$ for the GaAs-Al_xGa_{1-x}As heterostructure with $x \sim 0.2-0.3$ is $\sim 40\%$ of the energy-gap discontinuity ΔE_g . This result is therefore in substantial agreement with the recent trend of determinations of Q_v for this system.³

II. EXPERIMENT

Both samples studied were grown on (100) Cr-doped GaAs substrates by molecular-beam epitaxy, with As₂-rich growth conditions and substrate temperatures of 675 °C. The half-parabolic potentials were obtained by chopping the aluminum molecular beam with a computer-controlled shutter to obtain the desired average potential as described in connection with earlier work.¹ This sample contained five wells with $L = 522 \pm 31$ Å and 229-Å-wide $x = 0.26 \pm 0.05$ alloy barriers. Each well consisted of 43 layers with layers $i = 1, 3, 5, \dots, 43$ being GaAs of deposited thickness $(L/22) \{1 - [(44 - i)/44]^2\}$. Layers $i = 2, 4, 6, \dots, 42$ were Al_{0.26}Ga_{0.74}As with deposited thickness $\approx (L/22) [(43 - i)/44]^2$. Gallium-arsenide and aluminum-gallium-arsenide growth rates were determined by measurement of deposited film thicknesses of GaAs and AlAs adjacent to a mask which cast displaced shadows for gallium and aluminum beams. The aluminum beam-flux intensity in the shuttering sequences was determined by independent measurement of aluminum flux with an ion gauge at the position of the substrate. Thicknesses of the individual periods in comparable structures were determined by cross-section examination by transmission electron microscopy and confirmed the periodicity, accuracy, and constancy to within $\sim 10\%$ of the determined values.⁴ The incremental effects of the principal residual sources of uncertainty in layer thicknesses, namely, interface roughness, beam-flux variations with time, and any

increase in the gallium sticking coefficient with aluminum content, are estimated to be small.

For the HPW structure the single-particle eigenvalues can be approximated by the following expression for infinitely high potential barriers:¹

$$E_{ni} = 2(n - \frac{1}{4}) \frac{\hbar}{L} \left(\frac{2Q_i \Delta E_g}{m_i^*} \right)^{1/2}, \quad n = 1, 2, 3, \text{ etc.}, \quad (1)$$

where $Q_i \Delta E_g$ gives the band offset for the i th particle at a point where the well has a width L . Since the structure is asymmetric, the corresponding wave functions have no parity. Note that in this approximation the $n = 1$ level is $\frac{3}{4}$ of the ladder spacing for $\Delta n = 1$ above the bottom of the well. An equivalent expression like Eq. (1) for full parabolic wells can be demonstrated to lead to energy-level spacings within a percent or two of those determined by an "exact" calculation encompassing the finite barrier height and the layer

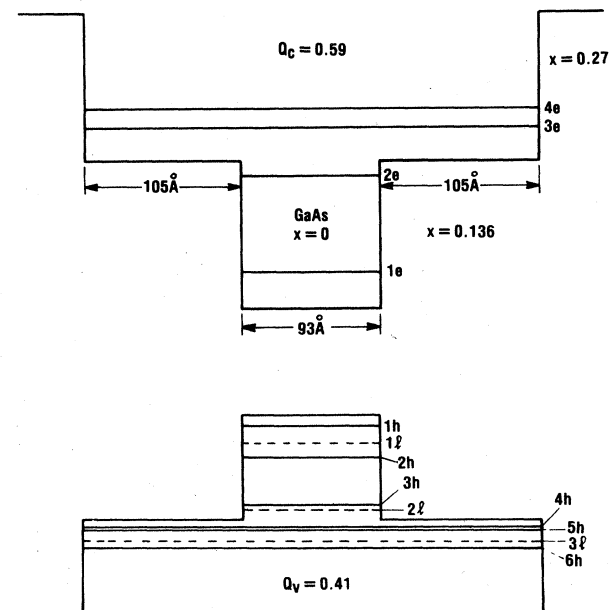


FIG. 1. The two-stepped quantum-well structure showing the relevant calculated single-particle levels with $Q_v = 0.41$.

configuration. The half-parabolic well structure has the potential advantage of exhibiting Δn even and odd interband transitions, and hence should yield direct determinations of the intraband energy-level spacings. The $\Delta n = 2$ transitions have been shown previously to be important in the determination of Q_i .^{1,2}

The two-stepped well is shown schematically in Fig. 1. It was designed so that the $n = 2$ electron level and the $n = 3$ heavy-hole level would be close to the top of their respective center wells with $Q_v \sim 0.4$ and hence be sensitive to the exact value of Q . These wells were grown using two Al ovens. Both shutters were open for the $x = 0.27$ alloy barriers which were 93-Å thick, and only one shutter open for the $x = 0.136$ alloy layers. The sample contained 20 periods.

A. Results

1. Half-parabolic wells

The excitation spectrum at 6 K for the HPW structure is shown in Fig. 2. To obtain the excitation spectrum, detection was set at ~ 1 meV below the photoluminescence (PL) peak at 1.53 eV and the incident photon energy scanned. The PL peak, not shown, is largely ground-state free-exciton emission and is ~ 3 meV full width at half maximum (FWHM). The most easily identified peaks, E_{1h} , E_{1l} , E_{12h} , E_{13h} , E_{2h} , E_{24h} , E_{3h} , E_{34h} , and E_{4h} , were used in the simple energy-difference analysis to determine the energy-level spacings. Exciton transitions, labeled E_{ij} , are for $\Delta n = 0$ transitions, where i denotes the electron and hole quantum numbers and j either a light (l) or heavy (h) hole. For $\Delta n \neq 0$ transitions E_{ijk} is used, where i and j are the quantum numbers for the electron and hole, respectively, and k denotes the hole character, l or h .

The electron and hole average energy-level ladder spac-

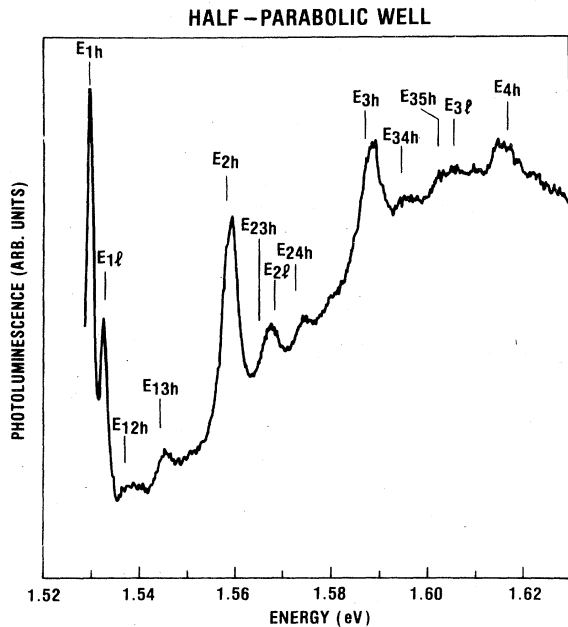


FIG. 2. The excitation spectrum at ~ 6 K for the half-parabolic well sample with detection set at 1.5285 eV and excitation at 0.3 W/cm² with a tunable dye laser. Calculated exciton transitions with $Q_v = 0.38$ are indicated by short vertical lines.

TABLE I. Experimental and calculated energy-level intervals for the half-parabolic well sample for electrons, heavy holes, and light holes, denoted by e , h , and l , respectively.

	Expt.	Eq. (1)	Exact
ΔE_e (meV)	21.6 ± 0.7	24.8	21.9
ΔE_h (meV)	7.4 ± 0.5	8.6	7.5
ΔE_l (meV)	13.6 ± 1.0	16.3	14.4

ings are given in Table I along with values calculated from Eq. (1) and those obtained via an "exact" calculation.¹ The exact calculation takes into account the 43-layer structure, the variation of effective mass with x , and the continuity of the wave function ψ_i and ψ_i/m_i^* at each heterointerface. The width of the HPW has been adjusted from the 522 ± 31 -Å estimate from the growth parameters to 548 Å to provide the best fit of the exact calculated values to the data. The (100) effective masses are the same as used previously,² namely, $m_e^*/m_0 = 0.0665$, $m_h^*/m_0 = 0.34$, and $m_l^*/m_0 = 0.094$. These hole masses are within the experimental uncertainties of the values given by Bimberg.⁵ The energy-level ladder spacings ΔE_i given in Table I for the electron, heavy hole, and light hole are denoted with $i = e$, h , and l , respectively. The calculated ΔE_i in Table I are for $Q_v = 0.38$. The fit with the actual data is indicated in Fig. 2 by the short vertical bars above the labeled transitions. The binding energy of the heavy-hole excitons $B_{1s}(h)$ was set equal to 8.0 meV to fit the observed E_{1h} and that for the light-hole excitons was assumed to be 9.0 meV.⁶ The average deviation of the calculated values from the experimental peaks is 0.7 meV with the largest deviation being 1.2 meV for E_{3h} . Thus the fit is excellent. Note that Eq. (1) gives values that are $\sim 8.5\%$ too high, whereas for the full parabolic wells we find the equivalent equation to be accurate to within $\sim 2\%$. The failure of Eq. (1) for the HPW is undoubtedly due at least in part to the penetration of the wave functions into the finite abrupt barrier with a consequent reduction of the eigenvalues.

2. Two-stepped wells

Figure 3 shows the PL and excitation spectra for the two-stepped quantum wells. In this case the PL contains a significant extrinsic component, as can be seen by the ~ 10 -meV Stokes shift from the E_{1h} exciton peak in the excitation spectrum. As with the HPW, the basic dimensions of the structure have been changed from the estimates based on growth rates to improve the fit of the calculated transitions to the data. In particular, the width of the central region was changed from 90 to 93 Å, and the upper well from 318 to 303 Å, the latter dimensions being used for Fig. 2.

Figure 4 shows the Q_c dependence of the calculated exciton transition energies for the more important expected transitions. To obtain these calculated curves, in each case the binding energy of the E_{1h} exciton $B_{1s}(h)$, was adjusted between 6 and 8 meV to fit the observed E_{1h} value, and $B_{1s}(l)$ was set equal to $B_{1s}(h) + 1$ meV. Also shown are the experimental transition energies including estimates of their uncertainties. As expected, the transitions with either electron or hole levels near the top of the central well are the most sensitive to Q . The calculation also suggests that

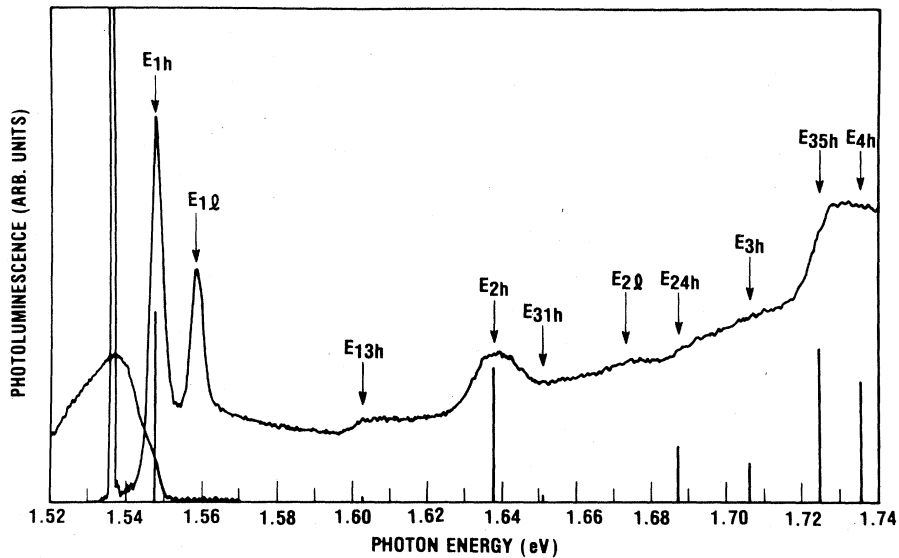


FIG. 3. The photoluminescence and excitation spectra at ~ 6 K for the two-stepped quantum-well sample described in connection with Fig. 1. The photoluminescence, shown in the left side of the figure, is largely extrinsic. For the excitation spectrum, detection was set at 1.537 eV and the exciting laser beam at ~ 3 W/cm² scanned in energy. The energies of the exciton transitions calculated with $Q_v = 0.41$ for the major relevant transitions are indicated by short vertical arrows below the transitions. Relative calculated strengths for the heavy-hole transitions are given by the vertical lines below the transitions.

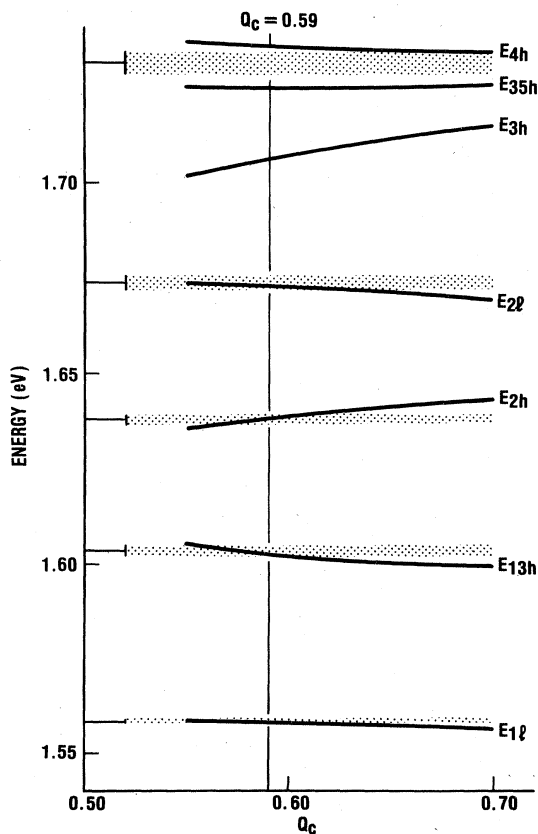


FIG. 4. The calculated exciton transition energies for the two-stepped quantum wells as a function of $Q_c = 1 - Q_v$. A value of $Q_c = 0.59$ gives the best fit to the experimental data.

E_{35h} and E_{4h} overlap in energy. The data are best fit by $Q_v = 0.41$. Computations based on the original estimates of the structure dimensions give the best fit for $Q_v \sim 0.42$, so that for this structure Q_v does not depend critically on the sample direction.

The calculated exciton transition energies using $Q_v = 0.41$ are shown in Fig. 3 by short arrows above the transition labels and are seen to be in good agreement with the easily identified transitions. The calculated single-particle levels are included in Fig. 1.

A more detailed comparison of the calculations with experiment should also consider the transition strengths. For example, to fit the data the calculated intensity for E_{3h} should be weak and that for E_{35h} strong, which is not the normal case for square wells. Thus, the strengths of the various heavy-hole transitions have been estimated using single-particle wave functions. This simple calculation does not take exciton effects into account, and has been shown previously to be questionable for some transitions, e.g., E_{13h} with square wells.¹ However, the results for parabolic wells demonstrate clearly the usefulness of this type of calculation.¹ To determine the transition strengths, the required wave functions were obtained by integrating Schrödinger's equation numerically. The relative calculated strengths for the heavy-hole transitions are indicated by the heights of the vertical lines at the transition energies. The E_{1h} , E_{2h} , E_{35h} , and E_{4h} transitions are estimated to be strong, as observed. The transitions E_{24h} and E_{3h} are estimated to have moderate strength, which is not inconsistent with the weak structure and rising signal level between E_{2l} and E_{35h} . Transitions E_{31h} and E_{13h} are expected to be very weak as is observed for E_{31h} , but E_{13h} is stronger than expected, as has been noted earlier for this particular transition.¹ In any event, the calculated strengths add support to the interpreta-

tion presented, which requires a relatively weak E_{3h} and a strong E_{3sh} overlapping with a strong E_{4h} .

III. CONCLUSIONS

The design of both structures leads to transitions, some $\Delta n=0$, and some $\Delta n \neq 0$, which play an important role in

determining the band offsets. The uncertainties in the Q values are difficult to estimate, but $Q_v=0.40 \pm 0.03$; hence $Q_c=0.60 \pm 0.03$ would encompass the present determinations and also an earlier one by the same authors.² These conclusions are relevant for GaAs-Al_xGa_{1-x}As interfaces with x in the range ~ 0.2 – 0.3 and are in good agreement with other recent determinations of Q_v .³

¹R. C. Miller, A. C. Gossard, D. A. Kleinman, and O. Munteanu, Phys. Rev. B **29**, 3740 (1984).

²R. C. Miller, D. A. Kleinman, and A. C. Gossard, Phys. Rev. B **29**, 7085 (1984).

³For a summary of band offset determinations, see W. I. Wang and F. Stern, in *Proceedings of the Twelfth Annual Conference on the Physics and Chemistry of Semiconductors*, edited by R. S. Bauer [J. Vac. Sci. Technol. **3**, 1280 (1985)].

⁴P. M. Petroff and D. Werder (unpublished).

⁵D. Bimberg, in *Festkörperprobleme*, edited by J. Treusch, *Advances in Solid State Physics*, Vol. XVII (Pergamon/Vieweg, Braunschweig, 1977), p. 195.

⁶C. Priester, G. Allan, and M. Lannoo, Phys. Rev. B **30**, 7302 (1984); R. C. Miller, D. A. Kleinman, W. T. Tsang, and A. C. Gossard, *ibid.* **24**, 1134 (1981).